

Laminar fine structure of frequency organization in auditory midbrain

Christoph E. Schreiner* & Gerald Langner†

* W. M. Keck Center for Integrative Neuroscience, Sloan Center for Theoretical Neuroscience, Coleman Laboratory, 513 Parnassus Avenue, University of California at San Francisco, San Francisco, California 94143-0732, USA

† Zoologisches Institut, Technische Hochschule Darmstadt, D-64287 Darmstadt, Germany

The perception of sound is based on signal processing by a bank of frequency-selective auditory filters, the so-called critical bands^{1–3}. Here we investigate how the internal frequency organization of the main auditory midbrain station, the central nucleus of the inferior colliculus (ICC), might contribute to the generation of the critical-band behaviour of its neurons. We find a unique spatial arrangement of the frequency distribution in the ICC that correlates with psychophysical critical-band characteristics. Systematic frequency discontinuities along the main tonotopic axis, in combination with a smooth frequency gradient orthogonal to the main tonotopic organization of cat ICC, reflect a layering of the frequency organization paralleling its anatomical laminae. This layered frequency organization is characterized by constant frequency ratios of corresponding locations on neighbouring laminae and may provide a spatial framework for the generation of critical bands and for signal processing within⁴ and across⁵ frequency bands for the analysis of sound.

Various perceptual phenomena indicate that the auditory system processes its inputs in the frequency domain by frequency-limited ‘critical bands’^{1,2}. The importance of a frequency-based sound analysis is reflected in the tonotopic layout of the majority of auditory nuclei. Although the concept of critical bands is of fundamental importance in psychophysics, the mechanisms underlying the generation of the corresponding physiological band-pass filters are unknown. These frequency bands represent narrow spectral ranges within which sound energy is integrated and are crucial for a sound’s perceived loudness², its detectability in background noise⁴, and its discriminability from other sounds. For example, two simultaneously presented pure tones may only be heard separately when located in different critical bands.

A neuronal theory of critical bands would have to account for two essential and invariant filter attributes: a logarithmic relationship between the filter’s bandwidth and centre frequency, and a level-independent bandwidth^{1,2}. It has been assumed that the filter processes of the auditory periphery are related to the critical-band concept³, but as the filter bandwidths of the cochlea and peripheral neurons are level-dependent and vary over a wide range^{6–14}, the required invariances of the critical-band filter can only be derived more centrally through processing mechanisms such as lateral inhibition. This mechanism creates level-tolerant filters in the central nervous system (CNS) of echolocating bats and has been encountered throughout the central auditory system^{15,16}. The lowest auditory station where neurons do have invariant filter properties comparable to critical bands is the ICC^{6–13}.

What features of ICC organization might contribute to the realization of critical band filters? The best-defined functional feature of organization of the ICC is the tonotopic representation of cochlear place or stimulus frequency^{17,18} along the dorsal–ventral extent of the ICC. Frequency mapping studies in the three dimensions of the ICC have led to the concept of functional ‘iso-frequency laminae’ orthogonal to the main tonotopic axis: that is, continuous sheets of neurons tuned to the same frequency that span the entire

ICC from edge to edge^{17–19}. Anatomical studies indicate that a prominent structural feature of the ICC is a preferred orientation of its principal neurons which are arranged in distinctive, parallel fibrodendritic laminae with a thickness of 120 to 180 μm (refs 20–25). In the cat ICC, this allows for 30 to 45 stacked anatomical laminae. They seem to be of functional significance because laminae defined by electrophysiology^{17–19,25,26}, by activity-dependent markers^{27,28}, or by neuroanatomical methods^{20–25} are of similar spatial orientation and extent.

We consider that a layered but largely continuous frequency organization exists in the ICC and that it is the neuronal substrate at which critical bands emerge. The spatial relationship of a laminated anatomical structure and a specific distribution of functional properties within and across laminae, such as complex local inhibition and integration networks, appears to be particularly suited for the generation and function of critical bands. If lamination helps to create critical bands, three conditions must be fulfilled: (1) frequency relationships between neuronal neighbours on adjacent laminae have to be correlated with the size of critical bands; (2) short-range inhibition between adjacent laminae has to

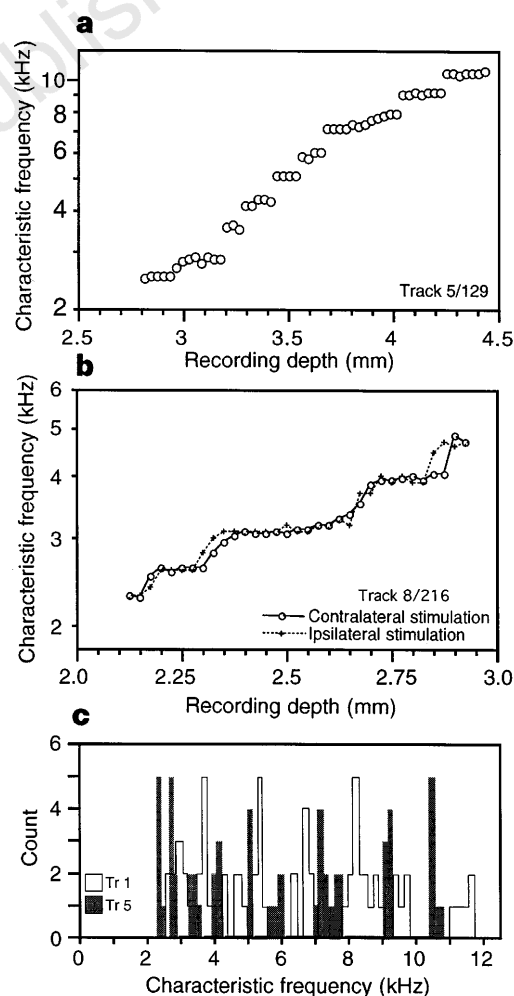


Figure 1 Stepwise progression of characteristic frequency (CF) along the main tonotopic axis in ICC. **a**, Example of a single electrode track with pronounced CF plateaux and steps. Note the similar step size on the logarithmic scale over 2 octaves. **b**, Example of CFs for contra- and ipsilateral stimulation. CF values obtained by stimulation of either ear are largely the same. Steps for the CF curves obtained for one ear may occur at slightly different depths from those for the other ear. **c**, Histogram of CF counts gathered from two parallel electrode tracks separated mediolaterally by $\sim 425 \mu\text{m}$. The histograms reveal a complementary frequency distribution by showing the same step sizes in the two penetrations but different frequency plateaux.

Figure 2 Spatial and frequency spacing of frequency plateaux along dorso-ventral electrode tracks in the ICC. **a**, Distribution of the change in recording depth from one frequency plateau to the next. The mean step size corresponds roughly to the spacing of anatomical laminae in the ICC²⁰⁻²⁵ (bar above the distribution). Only the spacing of consecutive frequency plateaux with at least three constant CF values each were included. **b**, Distribution of frequency step sizes in octaves. The range of behaviourally determined critical bandwidths^{8,9,34} (bar above the distribution) corresponds to the range of frequency steps. **c**, Frequency-dependence of step size. Circles represent frequency step size as a function of CF ($n = 8$ animals). Behaviourally determined critical bandwidths (CB) (open triangles⁸, filled triangles¹⁴) reveal the same trend and correspond to 1-2 frequency steps. Neuronal critical bandwidth (solid line represents average of bandwidth determined for single units with narrow-band noise masker⁷) matches the frequency dependency of the collicular frequency steps, as well as the behavioural data. The lower boundary of these neuronal data is similar to the behavioural as well as the frequency-step estimates of critical bands⁷⁰.

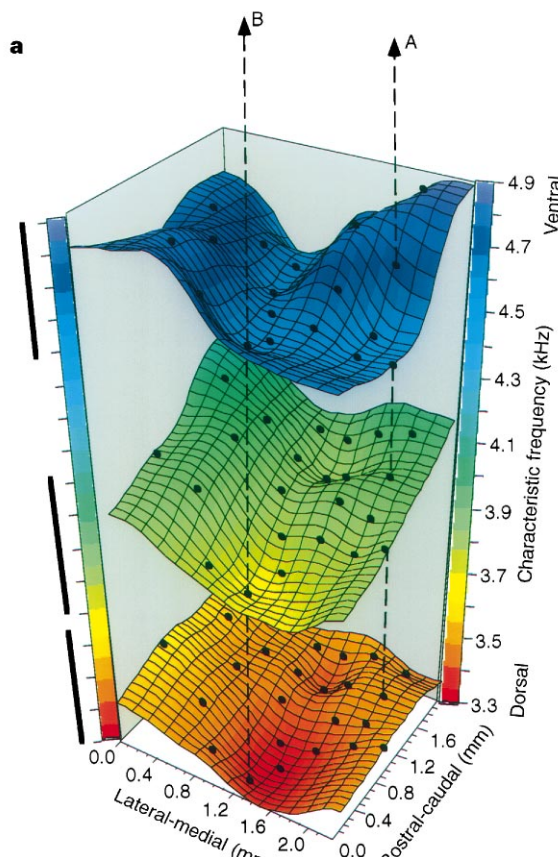
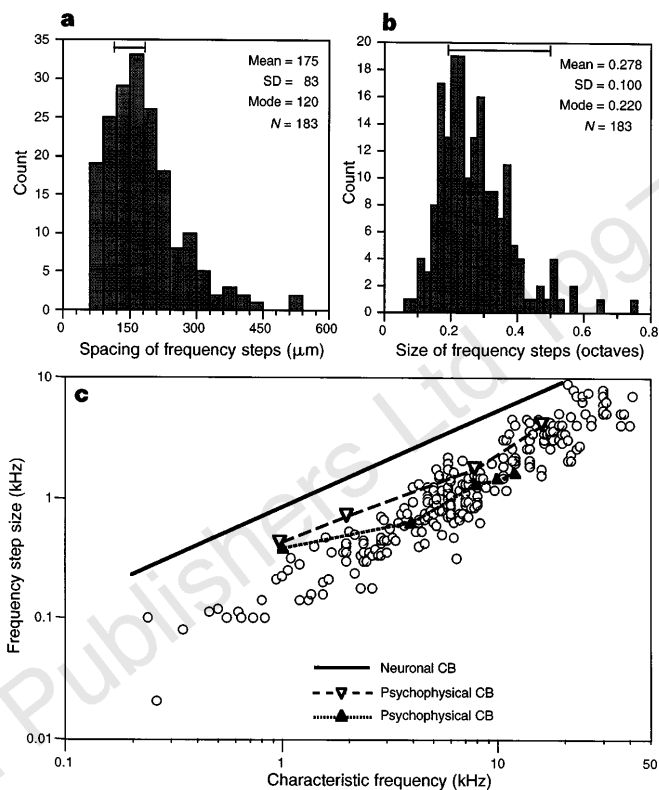
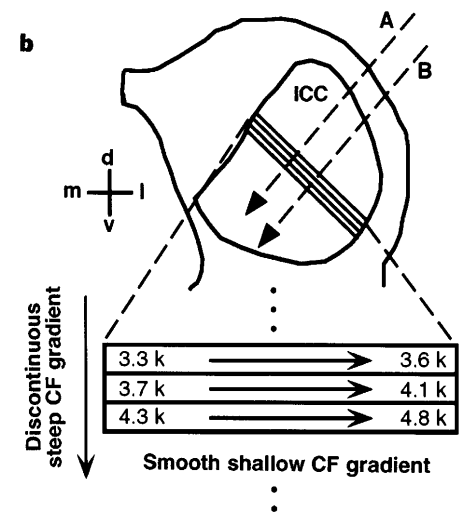


Figure 3 a, Reconstruction of functional frequency-band lamina in the ICC. Frequency representation in three adjacent frequency-band laminae was reconstructed from 23 parallel dorso-ventral electrode tracks in the ICC. The trajectory of two electrode tracks (A,B) is indicated by the arrows. The frequency content of each functional lamina was assigned by closest neighbourhood relation. Each lamina covers about 1/4 of an octave of non-overlapping frequencies (as indicated by the colour code and the bars on the left margin). In addition, for each lamina a small, approximately rostral-medial to caudo-lateral gradient of the tonotopic fine structure can be discerned with the aid of a pseudo-3D grid. Almost the full frequency range covered (3.3-4.9 kHz) is represented as the CF value on one of the 3 frequency-band laminae. The frequency gradient is not complete along the main dorsal-ventral tonotopic axis of the nucleus, but is



expressed as a layered sheet with a shallow gradient within each lamina and a steep gradient across laminae. The frequency gaps between the sampled frequency-band laminae are due to the fact the 23 tracks covered only ~4 mm² or ~2/3 of the total area of the full laminae. Given a systematic frequency representation within the laminae, not all expected CFs could be encountered in this incomplete mapping. **b**, Frequency gradients in the ICC. Arrows (A,B) indicate the trajectories of the corresponding example penetrations in **a**. Each schematic lamina displays the CFs at its lateral (l) and medial (m) edges for a fixed rostral-caudal location (0.4 mm). The full CF range within each lamina is slightly larger than indicated owing to an additional gradient in the rostral-caudal dimensions, and is ~3.1-3.7 kHz, 3.7-4.3 kHz and 4.3-5.2 kHz, respectively. d, Dorsal; v, ventral.

exist; and (3) the first two conditions have to be realized for each potential centre frequency of a critical band, that is, in principle, for all frequencies of the hearing range.

The second condition is probably fulfilled: inhibition between neurons in the ICC has been investigated in some detail and the existence of inhibitory connections between adjacent laminae has been demonstrated in bats and cats^{29,30}, although the precise role of inhibition on spectral receptive fields remains unclear. Anecdotal observation of discontinuities in the frequency representation^{17,18} suggests that the functional organization within the ICC might be related to its structural lamination^{25,27}. To reveal the potential relationship between laminae, frequency organization, and critical bands, a detailed analysis of the fine structure of the frequency organization in the dimension of the 'iso-frequency laminae' as well as along the main tonotopic axis is necessary.

The characteristic frequency (CF) of the locally most sensitive collicular neurons was obtained every 25–30 μm along latero-dorsal to medio-ventral microelectrode penetrations through the ICC of the cat. The estimated group characteristic frequencies for stimulation of either ear showed a global increase with recording depth in the latero-dorsal to medio-ventral direction, consistent with the previously defined tonotopic organization of the ICC^{17,18}. However, the progression of the characteristic frequency was not gradual, but discontinuous or stepwise^{17,18} over a large range of each penetration (Fig. 1). An analysis of the discontinuities revealed that the stepwise progression in the characteristic frequency sequence was characterized by two attributes: the spatial distance over which nearly constant characteristic frequencies were encountered, and the size of the frequency steps from one frequency 'plateau' to the next. The distance over which a given group of neurons dominated the characteristic frequency was $175 \pm 83 \mu\text{m}$ ($n = 183$) for penetrations that were roughly orthogonal to the orientation of the laminae (Fig. 2a). As the orientation of the laminae changes slightly with recording depth, the average distance measured in straight electrode tracks is larger than the actual distance between laminae. The relative stepwise increase of characteristic frequency was nearly invariant and, on average, 0.278 ± 0.100 octaves per frequency step (Fig. 2b) for the full audible frequency range. At CF = 4 kHz, for example, this corresponds to a step size of 0.8 kHz. Consequently, values of the characteristic frequency are not smoothly and completely distributed in penetrations along the main dorso-ventral tonotopic axis of the ICC but show a regularly spaced, discrete frequency representation.

Parallel electrode penetrations that were made close to each other (<300 μm) usually showed similar step sizes and plateau frequencies. In more widely spaced penetrations, the relative step sizes were also similar, but the plateau frequencies of the discrete frequency progression often differed by a small, constant amount. Accordingly, the frequencies encountered in more widely separated penetrations were systematically interspersed (Fig. 1c). It follows that the characteristic frequencies represented along a single dorso-ventral trajectory across the ICC do not continuously cover the complete frequency range. However, a non-quantal, complete characteristic frequency distribution can be established by combining all available dorso-ventral trajectories. The similar spacing of frequency discontinuities and fibro-dendritic laminae^{20–25} strongly suggests a correspondence between functional and structural laminar organization.

Additional support for a fine structure of the tonotopic organization in the ICC comes from a comparison of the characteristic frequency sequences for contra- and ipsilateral acoustic stimulation (Fig. 1b). Although the encountered characteristic frequencies along a given penetration generally matched for input from either ear, the depth location of the frequency discontinuities for the two ears were occasionally shifted by 30 to 90 μm . This suggests that binaural inputs of the same frequency are not always in perfect spatial register and provides physiological support for the anatomi-

cal finding that binaural inputs to the ICC may be spatially segregated^{20–25}.

These results confirm the hypothesis that the characteristic frequencies within a given lamina are not constant but change with location, and that the notion of 'frequency-band laminae' in the ICC is more appropriate than 'iso-frequency laminae'^{17–19}. More important, the findings show that neighbouring locations on adjacent laminae have a specific characteristic frequency ratio. The mode of these ratios was 0.22 octaves (for example, 4.66/4.0 kHz) which corresponds to ~ 0.5 –1 critical band in cats^{4,8,9,14} (Fig. 2c). Owing to the recording method, this finding only holds for low-threshold neurons and other groups of neurons may show deviations from this pattern^{19,21}.

The three-dimensional reconstruction of individual 'frequency-band laminae' revealed a systematic and continuous representation of a narrow frequency range within each lamina, manifesting as a gradient orthogonal to the main dorso-ventral tonotopic axis. The shallow gradient of this frequency representation is $\sim 0.09 \pm 0.04$ octaves mm^{-1} (Fig. 3a). The higher frequencies in the reconstructed laminae were generally located near the lateral edge of the nucleus and the lower frequencies near the rostral-medial edge (Fig. 3a,b). The frequency range across the extent of a lamina corresponds to the size of the frequency step to the next lamina.

These findings suggest the existence of a unique and precisely organized fine-structure of the frequency distribution in the ICC that consists of a segmented and layered characteristic frequency arrangement. In a stack of 30–45 frequency-band laminae (Fig. 3b), each exhibits a shallow, continuous frequency progression orthogonal to the traditionally defined main dorso-ventral tonotopic axis, and a more than ten-times steeper, but discontinuous frequency progression across the laminae ($\sim 1.6 \pm 0.7$ octaves mm^{-1} along the main tonotopic axis). We interpret this layered frequency organization as a potential structural substrate for the creation of critical bands by lateral inhibition. The ratios of the centre frequency of a neuron and of its neighbours on the two adjacent laminae is constant for all neurons, allowing reciprocal inhibitory interactions to shape the upper and lower boundaries of tuning curves appropriate for critical-band filters. The spatial relationships in the laminated frequency organization provide the necessarily constant relative bandwidths across the full range of audible frequencies. Accordingly, the three conditions deemed necessary for the generation of critical bands (see above) appear to be fulfilled by the layered fine structure of the tonotopic map in the ICC. Along the rostral-caudal extent of a frequency-band lamina, isofrequency contours (connecting locations of neurons with the same characteristic frequency) allow for the spatial representations of additional functional parameters. Consequently, the laminar organization of collicular neurons may be essential not only for the generation of critical bands but also for the extraction of information-bearing parameters for the perception of periodicity pitch and sound localization, as well as other perceptual attributes^{23,25,26}. □

Methods

The inferior colliculus (ICC) was exposed in 8 barbiturate-anaesthetized cats through a dorsal-lateral approach. Microelectrode penetrations were tilted laterally at a constant angle between 20° and 45° from vertical to achieve trajectories nearly orthogonal to the orientation of the anatomical laminae²¹. Multiple-unit responses were recorded every 25–30 μm and frequency response areas (FRAs) were reconstructed from 675 different level/frequency combinations. The characteristic frequency (CF) of the local group of neurons was defined as that frequency that produces the strongest neuronal response 5 to 10 dB above the lowest sound pressure producing any response. Accordingly, the CF data are biased towards the most sensitive local neurons. Often there were two response-threshold minima corresponding to two dominant CFs in the sampled cell population. With small advancement of the electrode, the CFs of the minima did not significantly change, whereas their threshold changed disproportionately with recording depth: one CF emerged at an increasingly

lower threshold and the other CF had an increasingly higher threshold. The occurrence at regular depth intervals of transitions from single-peaked to double-peaked tuning curves can be interpreted as a characteristic of functional lamination: single-peaked FRAs are representative of a spectrally uniform group of neurons within a functional lamina; double-peaked FRAs correspond to locations recording from neurons of two adjacent laminae. The fine spatial resolution necessary for defining a relationship between laminar and frequency organization, and the reconstruction of the frequency content of individual laminae, made it necessary to record activity from groups of neurons because it is not feasible consistently to isolate single neurons with the required spatial resolution. The same CFs and frequency steps were seen for advancing and retracting the electrode and for different electrode types.

A given 'frequency-band lamina' was reconstructed from the depth profile of several recording sites in three steps: (1) a CF plateau on a central penetration was chosen as the seed frequency for a functional lamina; (2) the horizontally closest penetration was selected and its CF plateau nearest to the seed frequency was determined, representing the most probable member of the same functional lamina as the seed frequency; (3) step 2 is repeated for the next nearest penetration until all penetrations have been included. Alignment for one lamina automatically defines the frequency content for all neighbouring laminae. In principle, the result of the alignment process does not depend on the initial seed frequency or penetration location.

Received 10 December 1996; accepted 2 May 1997.

1. Fletcher, H. Auditory patterns. *Rev. Mod. Physiol.* **12**, 47–65 (1940).
2. Zwicker, E. et al. Critical bandwidth in loudness summation. *J. Acoust. Soc. Am.* **29**, 548–557 (1957).
3. Greenwood, D. D. Critical bandwidth and the frequency coordinates of the basilar membrane. *J. Acoust. Soc. Am.* **33**, 1344–1356 (1961).
4. Watson, C. S. Masking of tones by noise for the cat. *J. Acoust. Soc. Am.* **62**, 167–172 (1963).
5. Yost, W. A. & Sheft, S. Across-critical band processing of amplitude modulated tones. *J. Acoust. Soc. Am.* **85**, 848–857 (1989).
6. Ehret, G. & Merzenich, M. M. Auditory midbrain responses parallel spectral integration phenomena. *Science* **227**, 1245–1247 (1985).
7. Ehret, G. & Merzenich, M. M. Complex sound analysis (frequency resolution filtering and spectral integration) by single units of the inferior colliculus of the cat. *Brain Res.* **13**, 139–163 (1988).
8. Pickles, J. O. Normal critical bands in the cat. *Acta Otolaryngol.* **80**, 245–254 (1975).
9. Pickles, J. O. & Comis, S. D. Auditory-nerve-fiber bandwidths and critical bandwidths in the cat. *J. Acoust. Soc. Am.* **60**, 1151–1156 (1976).
10. Ehret, G. Critical bands and filter characteristics in the ear of the house mouse (*Mus musculus*). *Biol. Cybern.* **24**, 35–42 (1976).
11. Ehret, G. & Moffat, A. J. M. Noise masking of tone responses and critical ratios of the mouse cochlear nerve and cochlear nucleus. *Hearing Res.* **14**, 45–57 (1984).
12. Pickles, J. O. Psychophysical frequency resolution in the cat as determined by simultaneous masking and its relation to auditory-nerve resolution. *J. Acoust. Soc. Am.* **66**, 1725–1732 (1979).
13. Evans, E. F. et al. Correspondence between behavioural and physiological frequency selectivity in the guinea pig. *Br. J. Audiol.* **23**, 151–152 (1989).
14. Nienhus, G. W. & Clark, G. M. Critical bands following the selective destruction of cochlear inner and outer haircells. *Acta Otolaryngol.* **88**, 350–358 (1979).
15. Suga, N. & Tsuzuki, K. Inhibition and level-tolerant frequency tuning in the auditory cortex of the mustached bat. *J. Neurophysiol.* **53**, 1109–1145 (1985).
16. Suga, N. Sharpening of frequency tuning by inhibition in the central auditory system: tribute to Yasuji Katsuki. *Neurosci. Res.* **21**, 287–299 (1995).
17. Merzenich, M. M. & Reid, M. D. Representation of the cochlea within the inferior colliculus of the cat. *Brain Res.* **77**, 397–415 (1974).
18. Roth, G. L. et al. Some features of the spatial organization of the central nucleus of the inferior colliculus of the cat. *J. Comp. Neurol.* **182**, 661–680 (1978).
19. Semple, M. N. & Aitkin, L. M. Representation of sound frequency and laterality by units in the central nucleus of the cat inferior colliculus. *J. Neurophysiol.* **42**, 1626–1639 (1979).
20. Rockel, A. J. & Jones, E. G. The neuronal organization of the inferior colliculus of the adult cat. I. The central nucleus. *J. Comp. Neurol.* **147**, 11–60 (1973).
21. Oliver, D. L. & Morest, D. K. The central nucleus of the inferior colliculus in the cat. *J. Comp. Neurol.* **222**, 237–264 (1984).
22. Oliver, D. L. Dorsal cochlear nucleus projections to the inferior colliculus in the cat: A light and electron microscope study. *J. Comp. Neurol.* **224**, 155–172 (1984).
23. Shneiderman, A. & Henkel, C. K. Banding of lateral superior olivary nucleus afferents in the inferior colliculus: a possible substrate for sensory integration. *J. Comp. Neurol.* **266**, 519–534 (1987).
24. Malmierca, M. S. et al. The central nucleus of the inferior colliculus in rat: A Golgi and computer reconstruction study of neuronal and laminar structure. *J. Comp. Neurol.* **333**, 1–27 (1993).
25. Chan, J. L. & Yin, T. C. T. Topographical relationships along the isofrequency laminae of the cat inferior colliculus: correlation with the anatomical lamination and representation of binaural response properties. *Soc. Neurosci. Abstr.* **8**, 348 (1982).
26. Schreiner, C. E. & Langner, G. Periodicity coding in the inferior colliculus of the cat. II. Topographical organization. *J. Neurophysiol.* **60**, 1823–1840 (1988).
27. Serviere, J. & Webster, W. R. A. A combined electrophysiological and [¹⁴C]-2-deoxyglucose study of the frequency organization of the inferior colliculus of the cat. *Neurosci. Lett.* **27**, 113–118 (1981).
28. Ehret, G. & Fischer, R. Neuronal activity and tonotopy in the auditory system visualized by c-fos gene expression. *Brain Res.* **567**, 350–354 (1991).
29. Pollak, G. D. & Park, T. J. The effects of GABAergic inhibition on monaural response properties of neurons in the mustache bat's inferior colliculus. *Hearing Res.* **65**, 99–117 (1993).
30. Palombi, P. S. & Caspary, D. M. GABA inputs control discharge rate primarily within frequency receptive fields of inferior colliculus neurons. *J. Neurophysiol.* **75**, 2211–2219 (1996).

Acknowledgements. Supported by the Office of Naval Research (C.E.S.) and the Deutsche Forschungsgemeinschaft (G.L.). We thank J. A. Winer for comments on the manuscript.

Correspondence and requests for materials should be addressed to C.E.S. (e-mail: chris@phy.ucsf.edu).

Kinesin hydrolyses one ATP per 8-nm step

Mark J. Schnitzer*† & Steven M. Block†‡

Departments of * Physics and † Molecular Biology, and ‡ Princeton Materials Institute, Princeton University, Princeton, New Jersey 08544, USA

Kinesin is a two-headed, ATP-dependent motor protein^{1,2} that moves along microtubules in discrete steps³ of 8 nm. *In vitro*, single molecules produce processive movement^{4,5}; motors typically take ~100 steps before releasing from a microtubule^{5–7}. A central question relates to mechanochemical coupling in this enzyme: how many molecules of ATP are consumed per step? For the actomyosin system, experimental approaches to this issue have generated considerable controversy^{8,9}. Here we take advantage of the processivity of kinesin to determine the coupling ratio without recourse to direct measurements of ATPase activity, which are subject to large experimental uncertainties^{8,10–12}. Beads carrying single molecules of kinesin moving on microtubules were tracked with high spatial and temporal resolution by interferometry^{3,13}. Statistical analysis of the intervals between steps at limiting ATP, and studies of fluctuations in motor speed as a function of ATP concentration^{14,15}, allow the coupling ratio to be determined. At near-zero load, kinesin molecules hydrolyse a single ATP molecule per 8-nm advance. This finding excludes various one-to-many and many-to-one coupling schemes, analogous to those advanced for myosin, and places severe constraints on models for movement.

Silica beads (0.5 μm diameter) were prepared with fewer than one molecule of kinesin, on average, bound nonspecifically to their surfaces. Beads were suspended in buffers containing variable amounts of ATP and introduced into a microscope flow cell. Individual diffusing beads were captured by an optical trap, deposited onto immobilized microtubules bound to the coverglass, and subsequent movements recorded with subnanometre resolution by optical-trapping interferometry^{3,13}. To ensure that beads were propelled by single molecules, they were prepared using extremely low concentrations of kinesin protein, sufficiently diluted from stock to make it unlikely that more than one molecule was present on a bead^{5,13}. In this regime, the fraction of beads moving as a function of kinesin concentration obeys Poisson statistics, confirming earlier findings^{4,5} (Fig. 1). To work at the lowest possible mechanical loads, the optical trap stiffness was set to just 7 fN nm⁻¹, producing a mean applied force of <0.9 pN in the optical trap (<15% of kinesin stall force¹³).

Average rates of kinesin movement were measured over three decades of ATP concentration. At saturating ATP levels, speeds were statistically identical to those measured by video tracking¹³ under no load, confirming the near-zero load condition. Speed data were well fit by Michaelis–Menten kinetics, with an apparent K_m for movement of $62 \pm 5 \mu\text{M}$ and k_{cat} of $680 \pm 31 \text{ nm s}^{-1}$, comparable to values found in microtubule gliding assays⁴ as well as solution studies of kinesin ATPase activity^{16–18}. This implies a Hill coefficient of one, and excludes models for movement that depart significantly from Michaelis–Menten kinetics¹⁹. Because hydrolysis activity in solution^{16–18} and speed *in vitro* display the same functional dependence on ATP, the coupling ratio—defined as the number of ATP molecules hydrolysed per mechanical advance—must be independent of ATP concentration. At limiting concentrations of ATP, k_{cat}/K_m gives a velocity of $11 \pm 1 \text{ nm s}^{-1} \mu\text{M}^{-1}$. In this regime, kinesin molecules advanced in clear increments of 8 nm (Fig. 2a), implying a stepping rate of $1.4 \pm 0.1 \mu\text{M}^{-1} \text{ s}^{-1}$ (Fig. 1). Statistical analysis of records, based on power spectra derived from pairwise distance differences⁵, revealed no signals corresponding to steps of